Voltage Distribution Characterization of CIGS Solar Cells Utilizing Luminescence Imaging Method

Rani Andhini Putri
andhini.putri@live.com

Instituto Superior Técnico, Universidade de Lisboa, Portugal
December 2016

Abstract
Defects in solar cells, such as series resistance or shunt resistance, can limit the efficiencies of solar cells. In order to improve energy production and energy efficiency in solar cells, luminescence imaging method is introduced. The luminescence imaging method is usually performed for quality control to help spotting local defects in solar cells. Luminescence is derived from the radiative recombination of electron and holes. This method is a non-destructive, fast, and versatile imaging method for spatially resolved solar cell and material characterization. There are two variants of luminescence imaging, which are photoluminescence (PL) and electroluminescence (EL). Since thin film cells are getting more attention in photovoltaic area, this thesis is focused on the characterization of $Cu(In,Ga)Se_2$ solar cells. CIGS solar cells emit radiation that is captured by a camera while operates at forward electrical bias, a method known as electroluminescence (EL). Through EL images, voltage distribution can be obtained. In this thesis, Haunschild's method of voltage-mapping is used, where two EL images were taken at different voltages to map the voltage distribution of the cell. Although Haunschild's method has been practiced on silicon solar cells, the aim of this thesis is to transfer the method used in Silicon solar cell to thin films. The measurements were carried out on on a small cell, which later will be upscaled to a larger cell.

1. Introduction

Luminescence imaging has recently been demonstrated to be fast experimental technique that allows measurement of the spatial distribution of the charge carriers' diffusion length in silicon solar cells and of the minority carrier lifetime in large area silicon wafers [1]. Luminescence imaging is a vital technique for quality control of the crystallization process to find defects, which limits the efficiencies of solar cells [1]. The advantage of luminescence imaging method is to help visualize and spot local defects, which limit the efficiencies of the solar cells. Defects such as shunts and series resistance can be seen through luminescence images. Another advantage of these techniques is that data acquisition times for high-resolution luminescence images are typically on the order of only seconds. Inspection of solar cells and panels during production can improve the quality, lifetime and energy conversion efficiency. When inspection takes place from the earliest moments in production, it helps pick out the downgraded solar cell material before it can get added value through later stages of manufacturing or cause machine downtime from parts broken due to defects. It is, therefore, a huge benefit in utilizing these methods in the fabrication process of solar cells, even modules, in order to achieve high efficiency [3].

Numerous studies and experiments have been carried out for silicon solar cells, while there have been limited number of research regarding spatially resolved electroluminescence (EL) and photoluminescence (PL) of thin films [4]. The conversion of these luminescence images into absolute quantities is the main area of research of this thesis. EL procedures were performed on CIGS solar to obtain quantitative results of the cell's voltage distribution. But the ultimate main goal of this thesis is devoted to the characterization of voltage distribution in solar cells through EL procedure. Hence, this thesis will strongly emphasize on EL rather than PL. Thesis objectives are met by the development of interpreting luminescence images in terms of local voltage.

2.Theory

Luminescence radiation is the energy released in the form of light from the recombination of electron and hole. In photoluminescence (PL), excess carriers (electrons and holes) are photo-excited by exposure to a sufficiently intense light

source, and the luminescence emitted from the radiative recombination of these photo-excited carriers. Electroluminescence (EL) is similar to PL, except that in electroluminescence the excess carriers are produced by current injection [5]. Emission of photons as a result of band-to-band radiative recombination is a common phenomenon observed in a direct band gap semiconductor, such as CIGS cells [4]. Therefore, this thesis concentrates on the characterization of CIGS solar cell.

The intensity of the emitted photons is related to the radiative band-to-band recombination method, material and optical properties of the cell material but there is a strong dependence on the applied voltage. The voltage mapping of a solar cell will give a better understanding of the series resistance, hence, EL images can be converted into voltage distribution image. The approach used in this thesis to compute voltage mapping is Haunschild's method, since it requires only two EL images taken at different voltages.

Haunschild et al. makes use of the relation between the local EL emission $\Phi_{el}(E)$ and the local junction voltage [6]. The combination of equation (1) and equation (2) gives the measured local luminescence in the EL case. In these equations, exponential function local voltage V_i can be taken out of the integrals, and when combined, the local luminescence is expressed as below,

$$\emptyset i = Ci * \exp\left(\frac{Vi}{Vt}\right) \quad (1)$$

Assuming injection independent charge carrier recombination properties, the local luminescence signal $\emptyset i$ at pixel $i = (x, y)$ scales exponentially with the local internal voltage Vi and it is also proportional to $\exp(\frac{Vi}{Vt})$, with Vt as the thermal voltage, Ci is the calibration constant which is related to optical and material properties of the camera and solar cell. This equation holds for conditions where Vi is larger than Vt [6]. The Ci relates the local luminescence intensity to the local junction voltage and is determined under low current injection or applied voltage conditions for EL. In this case, voltage gradients are negligibly small (due to the assumption of low resistances under low injection) and the local internal voltage Vi can be assumed equal to the applied voltage V_{appl} for every position of the cell. This procedure usually requires long integration time for the current to be distributed throughout the sample and it is assumed to be homogeneous [7]. Once Ci is calculated from the low power image, this calibration constant is then used to calibrate images at any excitation level to find its local junction voltage by

$$Vi = Vt * LN(\frac{\emptyset i}{Ci}) \quad (2)$$

However, this method has been practiced on the silicon solar cells and in this thesis, the aim is to transfer this methodology to CIGS thin film solar cells.

CIGS device structure

A typical CIGS thin film layer consists of six layers :

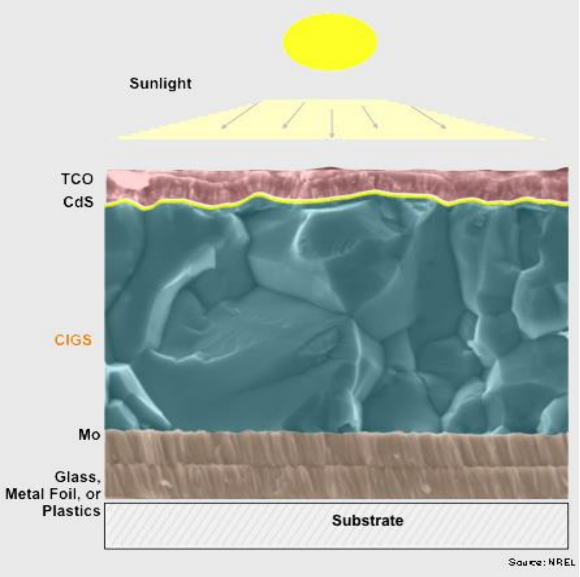

Figure 1: CIGS device structure [8]

A. Glass, Metal Foil, or Plastics
The glass functions as a substrate to support the thin solar cells. At Solliance, the glass used is soda lime glass (SLG) for about 1-3mm thickness. SLG is used mainly for the reason because it is relatively cheap and contains both sodium and potassium. The purpose of using sodium is to improve the electronic properties of the absorber. [8]

B. Molybdenum (Mo)
Moreover, this layer shows good conductivity, acceptable adhesion, have reasonably smooth and allow beneficial sodium diffusion that is necessary for the formation of good CIGS absorber.

Usually, Mo layer is around 0.3-1μm in thickness. [8]

C. CIGS
The absorber, CIGS, acts as the P-type material and has a thickness of 1-3μm. Light is absorbed and electron-hole pairs are created. This layer consists of copper indium gallium diselenide, which has a direct bandgap and a high optical absorption coefficient. Used in this thesis, the absorber is deposited by the vacuum co-evaporation. [8]

D. Cadmium Sulfide
The buffer, CdS, acts as the N-type and added on top of the absorber. CdS serves as a buffer layer because many of its physical properties, e.g. bandgap and refractive index are between those of the ZnO window layer and CIGS absorber layer. The CdS deposition provides a complete covering of the rough CIGS surface and a good passivation of the CIGS/CdS interface. CdS is normally deposited via chemical bath deposition and has a thickness of 50nm. [8]

E. Transparant Conductive Oxide
The standard sequence of the window layer TCO front electrode in this device consists of 50nm of intrinsic zinc oxide (i-ZnO) and 150nm of aluminum doped (ZnO:Al). The i-ZnO has a highly resistive material and it is used to prevent the establishment of shunt paths within the solar cells. The role of the i-ZnO layer in the CIGS device is discussed in Ref. [9], in which the authors discussed that the local series resistance provided by the i-ZnO mitigates the effects of the electrical inhomogeneities that limits the open-circuit voltage of the device. I-ZnO usually deposits by RF sputtering. Meanwhile, the Aluminum-doped ZnO (ZnO:Al) n-type semiconductor is transparent and conductive. This layer needs to be transparent to enable light to penetrate through the CIGS absorber layer. It also needs to be conductive to transport the electrons. This layer is deposited by RF sputtering method. [8]

F. Current Collecting Grid
To assist the collection of the produced current, metallic grids are applied on top of the TCO. Current collecting grids can either be thermally evaporated through micro structured shadow masks, made by lithographic methods, or printed. Larger amounts of metal in the grids typically provide better conductivity and, as a result, the efficiency losses due to an increase of the cell dimension are smaller. The efficiency of a metal grid current collector is determined by the conductivity of the metal grid and the distance between the grid lines [10].

3. Measurements

With the Greateyes system, EL procedure is performed on a CIGS cell with an area of 0.5cm^2. According to the procedure, a low power image is needed to obtain a calibration constant. To choose the low current to be injected to the cell, in this thesis is assumed to be 10% of the short circuit current of the cell. This CIGS sample has I_{SC} of 16mA; therefore, current of 1.6mA is injected to the cell (with a reading of voltage of 581mV) for 70 seconds. As said before, long integration time is necessary for low current to distribute a constant voltage across the cell. From Fig. 2 of low power image, gray value defines as the counts. It is visibly noticeable that the luminescence signal throughout the cell is constant and it is proven by the signal profile that is taken at the center of the cell. When the current injected is small, the voltage drop can be considered negligible, thus, creating an even distribution of voltage across the cell. This step is important since the calibration constant Ci can be calculated from equation (1). In addition, this lower power image possesses a homogeneous signal, therefore, Vi can be assumed to be the voltage applied to the solar cell, which is 581mV.

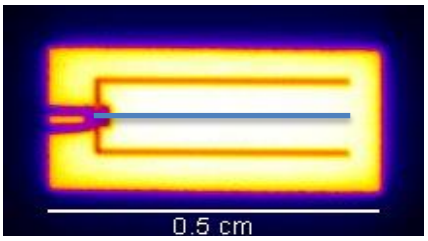

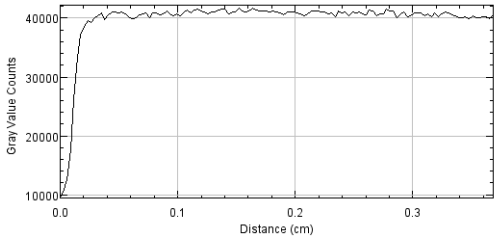

Figure 2: EL image of 1.6mA injection

The second measurement needed is the high power image. Fig. 3 is an EL measurement taken with 16mA injected and a voltage reading of 681.4mV for 5seconds. The high power image is needed to see the voltage-mapping image. As seen from the intensity profile, the signal decreases just after the busbar, which means, the high power image possesses high voltage drop, caused by the series resistance, yielding a non-homogeneous signal image. The goal is to be able to map the voltage distribution of the high power image.

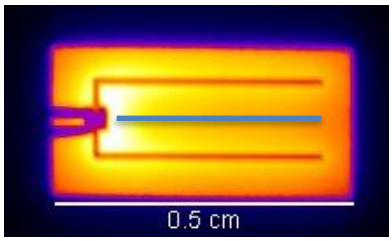

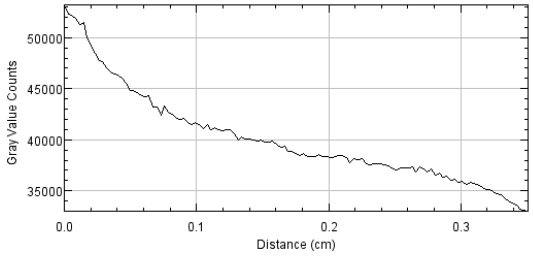

Figure 3: EL image of 16mA injection

As mentioned before, the low power image is used to calculate the Ci, with the condition $Vi = Vapplied$. This Ci is transferred to equation (2) for voltage distribution image. Fig. 4 shows the result from the calculation done on 1.6mA and 16mA images. However, the cell is barely visible since the upper part of the image has higher intensity than the cell.

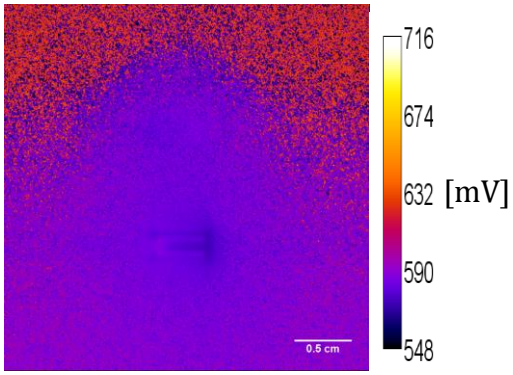

Figure 4: Local voltage mapping

The assumption of equation (1) was that the Vi is constant throughout the cell. However, during the calculation to find Ci using this equation, the whole image (including the non-active area) was taken into account and it was assumed to have a voltage applied of 581mV, when in fact the non-illuminating area had no voltage applied. Due to the error in the voltage distribution calculation, the non-active area shows a higher voltage than the cell. Essentially, the non-active area is not the area of interest, but due to this error, there is no visibility of the measured cell. Therefore, the signal of non-active area from the low power measurement should be altered in order to have approximately the same signal as the cell area.

The assumption of an equal voltage distribution throughout the whole cell was made for the low power measurement. Therefore, a modification image is only needed for the low power image. The modified image will change the non-illuminated area signal to be more or less the same as the cell's signal.

The procedure is to take the average value of signal from the center of the cell and set it as a reference, because it is assumed that the voltage on the center of the cell is constant. Then, if the signal of pixel position i is less than half of the reference, it will be replaced by the reference value. If not, the signal is unchanged. With this modification image, the non-active area would have the same signal as the average of the cell's intensity. The low power modification image is then used to calculate the calibration constant. Then, equation (2) is used to get the values of local voltage in every pixel i. Fig. 5 is the voltage distribution of 16mA using the modification image. With the modification of the low power image, the active cell area can be distinguished. The intensity is then adjusted to

display just the values from the minimum to the maximum intensity that the cell holds.

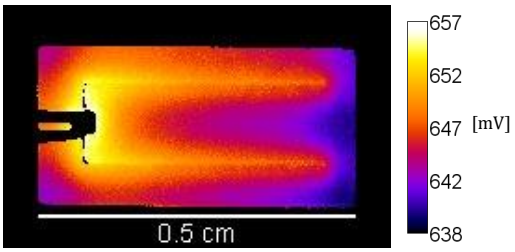

Figure 5: Voltage distribution of 16mA

The voltage distribution of 16mA injected has a voltage range of 638-657mV applied across the cell. However, when the measurement was done through injecting 16mA to the cell (for the high power measurement), the voltage reading on Keithley power supply showed 681.4mV. There is a 24mV difference between the voltage reading of Keithley and the calculated voltage. To evaluate and analyze the inaccuracy, a voltage difference test is done.

Voltage Difference Test

In order to analyze where the missing voltage goes, EL is performed on a single cell with current of 1.6mA, 3mA, 4mA, 6mA, 8mA, 10mA, 12mA, 14mA and 16mA. Using equation (1), 1.6mA is used as a calibration image, while equation (2) is used to perform voltage distribution calculation on the other images. From the data of the images, the maximum voltage from each image is obtained.

Table 1: Data for voltage difference

Current [mA]	Keithley [mV]	Image [mV]	Difference [mV]
3	602	600	2
4	613.8	606	7.8
6	631.2	620	11.2
8	644.5	631	13.5
10	655.5	639	16.5
12	665.1	646	19.1
14	673.7	652	21.7
16	681.4	657	24.4

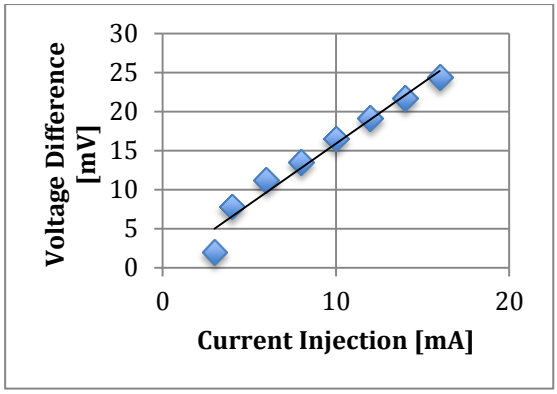

Graph 1: Voltage difference vs. Current Injection graph

As seen in Graph 1, it is clear that for higher current injection, the greater the voltage difference between the calculated and the measured values. With Ohm's Law, resistance can be calculated from each point, since there is a voltage difference between the calculated (reading from image) and the measured (reading from Keithley) at every current injection. For each current, the calculated resistance is around 1.5Ω to 1.8Ω. The difference between the calculated and the measured voltages is due to the series resistance within the cell or even from the contact resistance of the probes. However, it is highly possible that the back contact's (molybdenum) series resistance dominates it, which is not detectable by EL procedure, because the intensity gradient of the image through the use of EL shows the series resistance of the top surface of CIGS cell (TCO layer)

The non-uniformity of the luminescence signal is tightly related with the series resistance of the TCO. In the case of thin film solar cells, series resistance in TCO plays a crucial role in effective collection of photo-generated carriers (in other words, effective injection of minority carriers in EL measurement) to get high performance [11]. Therefore, it is not possible to determine the series resistance in the back contact, or the molybdenum for this case. However, the local determination of the series resistance is of greatest interest to solar cell analysis because the back and front contact, as well as the finger resistances make up the largest part of the total series resistance.

Scaling Up to Bigger Cells

The experiment has been done on a 0.5cm^2 CIGS cell for the purpose of trials. In the end, the

research was to conduct this method into different sizes of solar cells. Therefore, transferring the method into a larger area is essential. The new area that was experimented on is of 3cm^2 and 5cm^2.

For 3cm^2 area, the low power image needs to be injected with a small current with a longer integration time. With 8.3mA current injected in 200s, the voltage measured was 500mV. Meanwhile, the high power image is injected with current of 75mA in 3s, and the voltage was measured 800mV. The low power and high power image can be seen in Fig. 6 (a) and (b). The low signal (bottom left corner) on both Fig. 6 (a) and (b) illustrates the series resistance of the cell. However, the low power image can still be used since the signal gradient from high signal to low signal isn't that significant. Therefore, it can still be assumed that the voltage throughout the cell is constant. Using modified image, equation (1) and (2), the voltage mapping image is obtained.

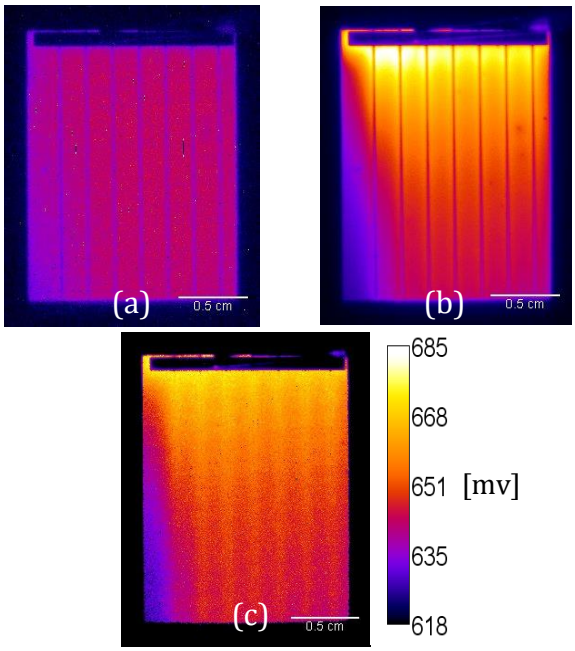

Figure 6: (a) Low power image, (b) High power image, and (c) Voltage mapping and its scale

Scaling up the area of the cell to 5cm^2 for EL procedure was predicted to be problematic for larger areas. Due to the low current that will not reach the end of the cell when applied on the busbar. Setting a long integration time for the procedure on a long cell would also give inaccuracy, since temperature of the system and the cell is related to the efficiency of the detector.

The assumption for calibration factor is to have approximately constant voltage throughout the cell, however, with a longer cell, this assumption may not hold. There would always be some resistances within the cell while injecting current through a long cell. Fig. 7 confirms that with EL itself, the low current injection is not possible to do with this 5cm^2 CIGS cell; cell was injected 10mA 500mV in 500s. The EL image shows noisy and non-homogeneous signal. Hence, it was hypothesized that a combination of PL and EL is needed to proceed with this experiment.

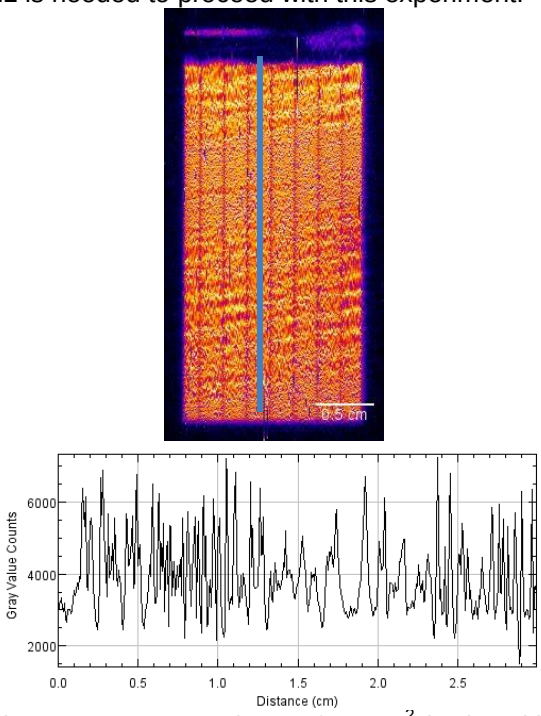

Figure 7: Low power image for 5cm^2 (top) and its intensity profile (bottom)

Combination of EL and PL

Fig. 8 (top) shows the PL image taken with LED power of 2A for 30 seconds. The LED power is set to a low intensity in order to provide low power image for calibration factor calculation. The calibration factor calculation requires a uniform signal, which represents a uniform voltage distribution since the intensity of the emitted photons depends on the applied voltage (in equation (1), V_i is assumed to be equal as voltage applied to the cell). Fig. 8 (bottom) displays the intensity profile of the image and it is evident that the cell possess a non-uniform distribution of signal. Meaning, this image cannot be used to calculate the calibration constant, since V_i is not equal to the voltage applied. V_{appl} was measured by Keithley to be in the range of 630-638mV, which proves that V_i cannot be

constant. In conclusion, this procedure is also challenging since the image that is required to calculate a calibration constant needs to have a constant voltage, allowing a negligible amount of series resistance. In addition, the uniformity of light causes an additional problem, since the LEDs are adjustable, it is possible that the emission of the light is not as homogeneous. The signal differs from 40000 counts to around 24000 counts. Therefore, PL/EL method is not a reliable method to use when scaling up the solar cell.

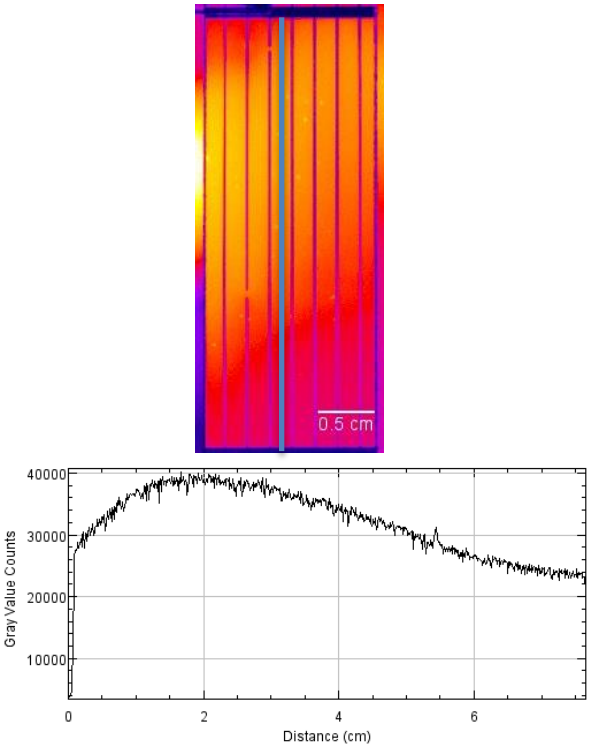

Figure 8: Low power image using a combination of PL and EL (top) and its intensity (bottom)

4. Conclusions, Discussions and Future Work

We have analyzed and demonstrate that voltage-mapping procedure of silicon solar cell can be transferred to thin film cells. This procedure is done using equation (1) to produce a calibration constant from a low power image with the assumption of a homogeneous voltage distribution; and equation (2) is used to calculate the voltage distribution of the high power image. But, there is a voltage difference between the measured (reading of Keithley) and calculated (scale bar of voltage image) maximum voltage. We are assuming that the series resistance within the CIGS causes the voltage difference between the calculated image and the voltage that is measured by Keithley. However, there is a strong possibility that the main resistance comes from the back contact. Furthermore, while this EL method is confirmed for small thin films ($0.5cm^2$ – $3cm^2$), transferring this method to long thin film cell above $5cm^2$ area was not successful. Series resistances are still dominating while doing low injection of EL procedure, in a short or long integration time. Thus, a combination of EL and PL was needed, in the aim to get a homogenous signal throughout the cell. Unfortunately, this procedure also gives a non-homogeneous signal throughout the cell. Therefore, silicon's voltage-mapping procedure can be transferred to small thin films but cannot be scaled up to a large area.

Future work regarding this thesis is to develop a new method of calibration constant that is based on non-homogeneous signal thin films. The voltage-mapping depends on the calibration constant that is required a homogeneous signal. Therefore, it is important to tackle the calibration constant for non-uniform signal. Afterwards, transforming the voltage-mapping to a series resistance image would be essential, since the series resistance has a great effect on the luminescence intensity. This would give us more degree of freedom in the analysis of the homogeneity of the thin films.

References

[1] Takashi Fuyuki, Hayato Kondo, Tsutomu Yamazaki, Yu Takahashi, and Yukiharu Uraoka, "Photographic surveying of minority carrier diffusion length in polycrystalline silicon solar cells by electroluminescence," *Applied Physics Letters*, vol. 86, p. 262108, 2005.

[2] Hinken, Karsten Bothe, and David, "Quantitative Luminescence Characterizaiton of Crystalline Silicon Solar Cells," in *Advances in Photovoltaics Part 2*, Gerhard P. Willeke and Eicke R. Weber, Ed., vol. 89, pp. 259-339.

[3] S. Fischer et al., "Enhancement of silicon solar cell efficiency by upconversion: Optical and electrical characterization," *Applied Physics*, vol. 108, p. 044912, July 2010.

[4] Torben Potthoffy, Karsten Bothe, Ulrich Eitner, David Hinken, and Marc Kontges, "Detection of the voltage distribution in photovoltaicmodules by electroluminescence imaging," *PROGRESS IN PHOTOVOLTAICS: RESEARCH AND APPLICATIONS*, vol. 18, pp. 100-106, January 2010.

[5] Thi-Minh-Hang Tran, "Quantitative analysis of spatially resolved electroluminescence of CIGS and a-Si:H thin-film solar cells and modules," Julich Forschungszentrum, Dissertation.

[6] MaxMile. Max Mile Technologies. [Online]. http://www.maxmiletech.com/applicationnotes/ELvsPL.pdf. [accessed on 27.10.2016]

[7] Jonas Haunschild, Markus Glatthaar, Martin Kasemann, Stefan Rein, and Eicke R. Weber, "Fast Series resistance imaging for silicon solar cells using electroluminescence," Phys. Status Solidi RRL 3, 2009.

[8] Markus Glatthaar et al., "Spatially resolved determination of dark saturation current and series resistance of silicon solar cells," 2010.

[9] Mirjam Theelen, *Degradation of Solar Cells*. Delft, 2015.

[10] M. Schmidt and U. Rau, "Electronic properties of ZnO/CdS/Cu(In,Ga)Se2 solar cells - aspects of heterojunction formation," *Thin Solid Films*, vol. 387, pp. 141-146.

[11] Yulia Galagan, Birger Zimmermann, Erica W.C. Coenen, and Mikkel Jørgensen, "Current Collecting Grids for ITO-Free Solar Cells,".

[12] Fuyuki, Ayumi Tani, and Takashi, "Direct Assessment of Series Resistance in Thin Film Solar Cells Utilizing Electroluminescence," Nara Institute of Science and Technology ,.